Paper No. 1369. (quote when citing this article)
Eleventh World Conference on Earthquake Engineering
ISBN: 0 08 042822 3
11 WCEE

DUCTILITY OF SHORT SPAN RC BEAMS

TOSHIYUKI KANAKUBO[*1], MASAMI FUJISAWA[*2], NORIMICHI SAKO[*3]
and YASUHISA SONOBE[*4]

*1: Institute of Engineering Mechanics, University of Tsukuba
1-1-1, Tennohdai, Tsukuba-city, 305, Japan
*2: Department of Architectural Engineering, Tsukuba College of Technology
4-3-15, Amakubo, Tsukuba-city, 305, Japan
*3: Technical Research Institute, Daisue Cooperation
6-8-10, Fukushima, Fukushima-ku, Osaka-city, 553, Japan
*4: Department of Architecture, Ashikaga Institute of Technology
268-1, Omae-cho, Ashikaga-city, 326, Japan

ABSTRACT

To investigate the ductility of short span RC beams, 16 specimens with shear span ratio of 1.2 or 1.4 were loaded cyclically using antisymmetrical loading system. The test parameters are type of concrete, concrete compressive strength, yield strength of stirrups and stirrup ratio. From the test results, yielding of longitudinal bars is observed in the most specimens. The observed failure modes are shear tension, shear compression and bond splitting. All specimens have a good ductility with no remarkable deterioration of loading stage until the translational angle, R =1/33 radians. The effective stress ranges of stirrups are about 700 - 800 MPa from the measured strain. The bending strength calculated by the e-function method can be adapted to evaluate the observed maximum loads. The critical ductility angles are also confirmed by using the shear capacity index.

KEYWORDS

RC beam; short span; antisymmetrical loading; ductility; failure mode; critical ductility angle; shear capacity index; bond capacity index

INTRODUCTION AND OBJECTIVES

Tube type reinforced concrete buildings have often been constructed for high-rise apartment house because of the increment of useful space, the freedom of plan arrangement and so on. As shown in Fig. 1, columns of tube type building are usually arranged to set along the building shell with a short span length such as about 3 meters or so. Therefore, this type of building has short span beams along the shell. As in the special case, shear span ratio of these beams sometimes becomes almost 1. It is necessary that these beams behave with good ductility under the earthquake force to let the building not fail.

Up to now, short span beam specimens have been usually used to research the shear strength and performance under the shear loading action, experimentally. These specimens are always designed not to have a yielding of main bars before shear failure. However, in actual frame type buildings with strong columns and weak beams, beams are allowed to have a yielding by bending moment. It is the most important point that how the beams behave after yielding. The main objective of this research is to investigate the performance of short span beams after yielding. In addition to this, a method to evaluate the ductility of short span beams is also discussed. To reach these objectives, the antisymmetrical loading test is carried out for 16 specimens of half scale models.

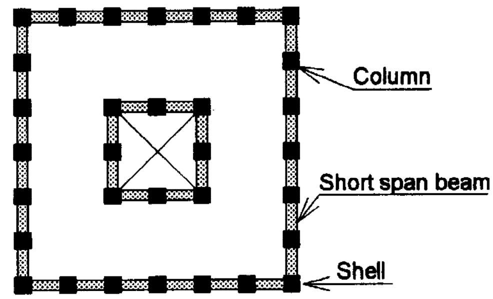

Fig. 1 A typical plan of tube type building

TEST PROGRAM

Loading Method and Measurements

The cyclic load is provided for all specimens using the antisymmetrical loading system as shown in Fig. 2. Specimens are set vertically at the central position of the system, and the shear force is applied by the 500 kN oil jack. As the loading beam is kept horizontally by the left side pantograph, the antisymmetrical deformation is to be applied to the specimen. The loading is carried out by controlling translational angle (*R*), defined as shown in Fig. 2. The loading history to be applied to all specimens is $R = \pm 1/200$, $\pm 1/100$, $\pm 1/50$, $\pm 1/33$ radians twice and $R = \pm 1/20$, $+1/15$ radians once.

Shear force, relative displacement between the upper and the lower stub and strains of reinforcements are measured.

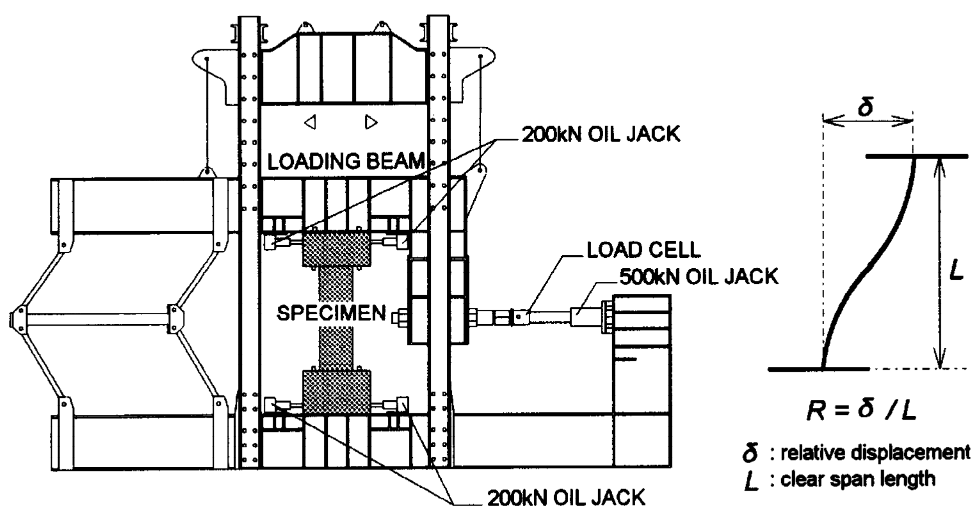

Fig. 2 Loading system

Specimens and Materials

16 specimens are tested. Dimensions of typical specimens are shown in Fig. 3. The cross section is 240 mm in width and 350 mm in depth, designed at a half scale of actual size beams. Clear span length is 840 or 980

mm, and shear span ratio (*M/QD*) is 1.2 (Series 1) or 1.4 (Series 2), respectively. The test variables are the arrangement of longitudinal bars (only parallel longitudinal bars or with diagonal ones), the amount and yield strength of stirrups, compressive strength of concrete (36 or 60 MPa class), and concrete type (light-weight concrete or normal-weight concrete). The relationships between these variables and the identification of each specimen are shown in Fig. 4. Mechanical properties of reinforcements and concrete are shown in Table 1.

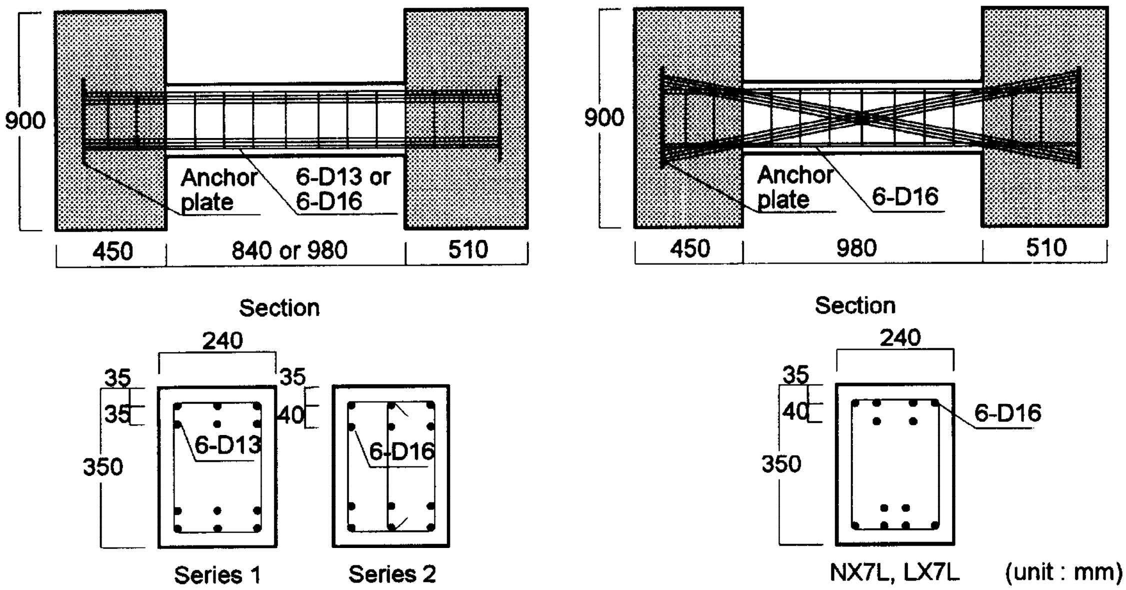

Fig. 3 Dimensions of specimens

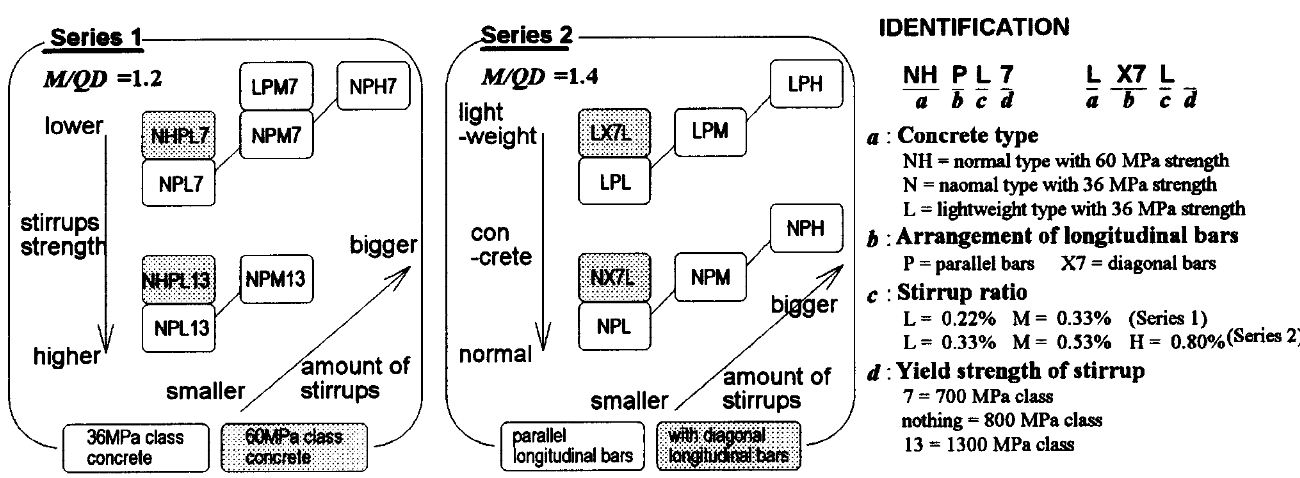

Fig. 4 Test variables and identification

Table 1 Mechanical properties of materials

Reinforcements					Concrete				
Type	Yield strength (MPa)	Tensile strength (MPa)	Young's modulus (GPa)	Remark	Type	Com-pressive strength (MPa)	Splitting strength (MPa)	Young's modulus (GPa)	Remark
D16	528	684	178	longt bar	Normal	38.1 - 45.3	2.81 - 2.98	21.0 - 23.2	36 MPa class
D13	550	700	182	longt bar					
D6	783	974	196	stirrup	Normal	78.5 - 80.5	4.10	27.8	60 MPa class
D6	923	994	200	stirrup					
U6.4	1242	1333	186	stirrup	Light	37.7 - 38.1	2.93 - 2.95	16.9 - 17.2	36 MPa class

TEST RESULTS

Q - R Curve and Failure Progress

Typical shear force (Q) versus translational angle (R) curves and final crack patterns are shown in Fig. 5. The failure progresses until the loading cycle to $R = \pm 1/100$ radians were almost the same in all specimens. First, bending cracks took place at the both ends of beams and they expanded as the displacement became larger. Next, shear cracks took place at the central portion of beams. In the most of specimens, yielding of longitudinal bars (F) is observed at $R = 1/150 \sim 1/100$ radians. Three types of failure modes are recognized, those are shear failure (ST), shear compression failure (SC) and bond splitting failure (BO). In general, the specimens failed by ST or BO showed remarkable decrement of load at loading cycle to $R = \pm 1/33$ radians. On the other hand, specimens failed by SC showed good ductility until $R = \pm 1/20$, and specimens with diagonal bars did not show a decrease of load at all.

Observed Strengths and Ductility

Table 2 shows the summary of test results and calculated values. Each term is defined as follows:

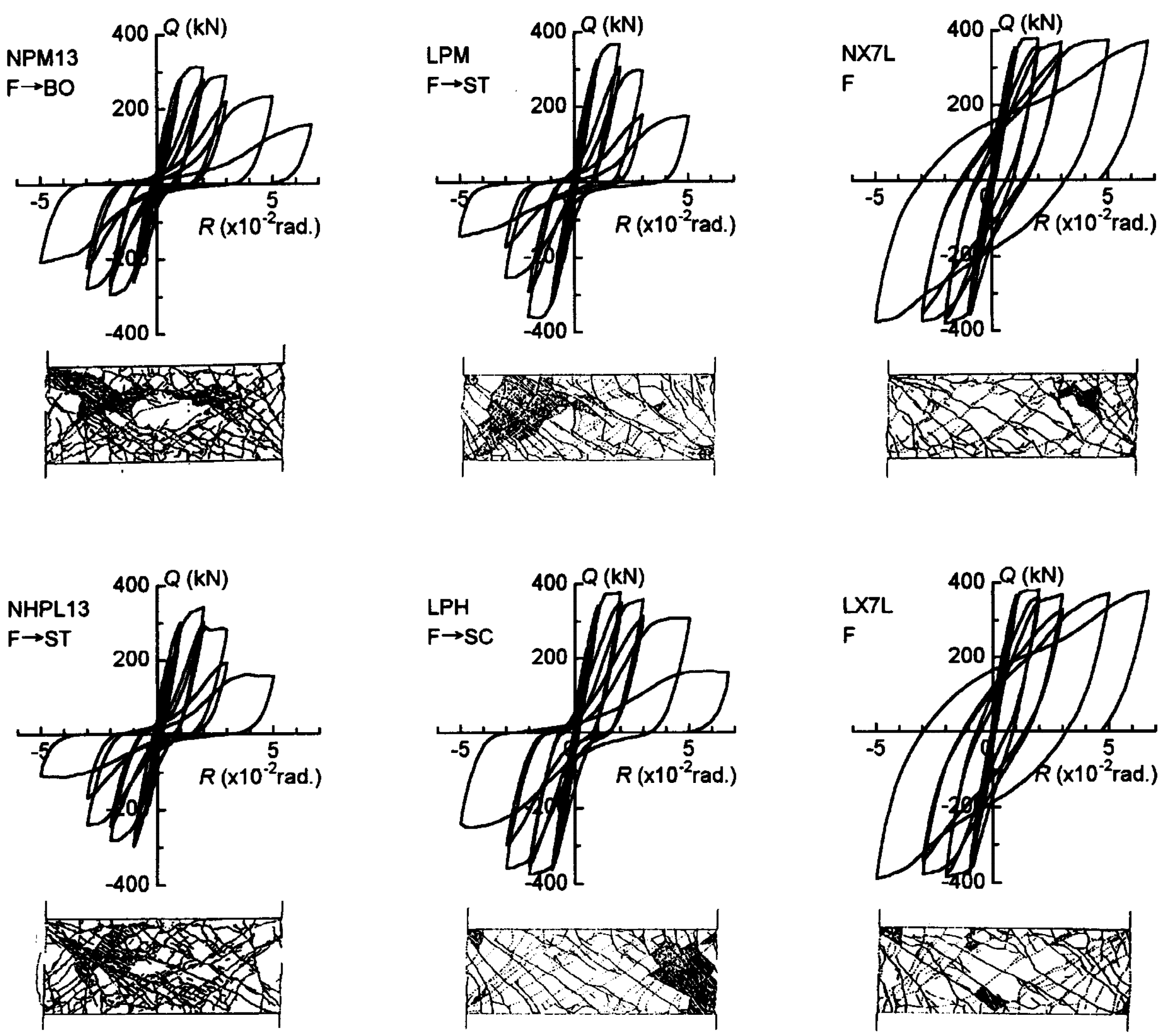

Fig. 5 Q - R curves and final crack patterns

Table 2 Calculated values and test results

Specimen	Calculated value			Result			
	Bending strength	Shear capacity index	Bond capacity index	Maximum load		Critical ductility angle	Failure mode
	$_cQ_{mu}$ (kN)	$_cQ_{su}$ / $_cQ_{mu}$	$_cQ_{bu}$ / $_cQ_{mu}$	$_eQ_{max}$ (kN)	$_eQ_{max}$ / $_cQ_{mu}$	$_eR_u$ (x 0.01 rad.)	
NPL7	284	1.07	1.27	267	0.94	3.05	F → BO
NPM7	284	1.30	1.31	300	1.06	4.88	F → SC
NPH7	277	1.63	1.55	302	1.09	5.01	F → SC
NPL	339	0.98	0.82	338	1.00	2.09	ST, BO
NPM	341	1.31	1.30	360	1.05	3.01	F → BO
NPH	341	1.49	1.35	381	1.11	4.87	F → SC
NX7L	345	1.69	1.03	365	1.06	> 6.69	F
NPL13	284	1.28	1.28	277	0.97	3.01	F→ST, BO
NPM13	284	1.59	1.31	303	1.07	5.00	F → BO
NHPL7	304	1.07	1.42	326	1.07	2.60	F → ST
NHPL13	305	1.30	1.42	332	1.09	3.00	F → ST
LPM7	277	1.27	1.51	261	0.94	1.40	F → ST
LPL	341	1.10	0.88	304	0.88	2.00	ST
LPM	341	1.40	0.98	355	1.03	3.01	F → ST
LPH	341	1.56	1.04	364	1.06	5.01	F → SC
LX7L	343	1.84	1.10	369	1.06	> 6.67	F

$_cQ_{mu}$: calculated bending strength by e-function method (Mutoh, 1967)
$_cQ_{su}$: calculated shear strength by truss-arch theory (AIJ, 1994)
$_cQ_{bu}$: calculated bond strength by Morita-Fujii's method (Morita et al., 1982)
$_cQ_{su}$ / $_cQ_{mu}$: shear capacity index
$_cQ_{bu}$ / $_cQ_{mu}$: bond capacity index
$_eQ_{max}$: observed maximum load
$_eR_u$: critical ductility angle = the translational angle when the peak load decreases less than 80% of the maximum load

Shear capacity index and bond capacity index are the calculated values introduced by authors to evaluate ductility and failure mode. Ideally, specimens which have shear capacity index smaller than 1 will fail by shear, and specimens with bond capacity index smaller than 1 will fail by bond. Critical ductility angle is treated as one of the indexes representing the ductility of specimens.

The observed maximum loads of specimens with yielding of longitudinal bars show a good correlation with calculated bending strength. The ratio of $_eQ_{max}$ to $_cQ_{mu}$ ranges from 0.94 to 1.11, and their average is 1.04. It is clear that the bending strength can be determined by the ordinary ways such as e-function method with regardless of shear span ratio.

Critical ductility angle generally increases, as stirrup ratio also increases in case of the specimens having the same concrete type. However, it is considered that the yield strength of stirrups has no influence to critical ductility angle. Fig. 6 shows examples of strain distribution of stirrups using 700 MPa class (NHPL7) and 1300 MPa class (NHPL13) reinforcements. In specimen NHPL7, strains which are bigger than yield strain are recognized from the loading stage of 1/100 radians. In specimen NHPL13, measured strains do not exceed yield strain, and the almost of them remain about 0.3 - 0.4 %. It is considered that the stresses of stirrups range from 600 to 800 MPa in case of the specimens used for this research. From the Table 2, critical ductility angle has better relationship with failure modes.

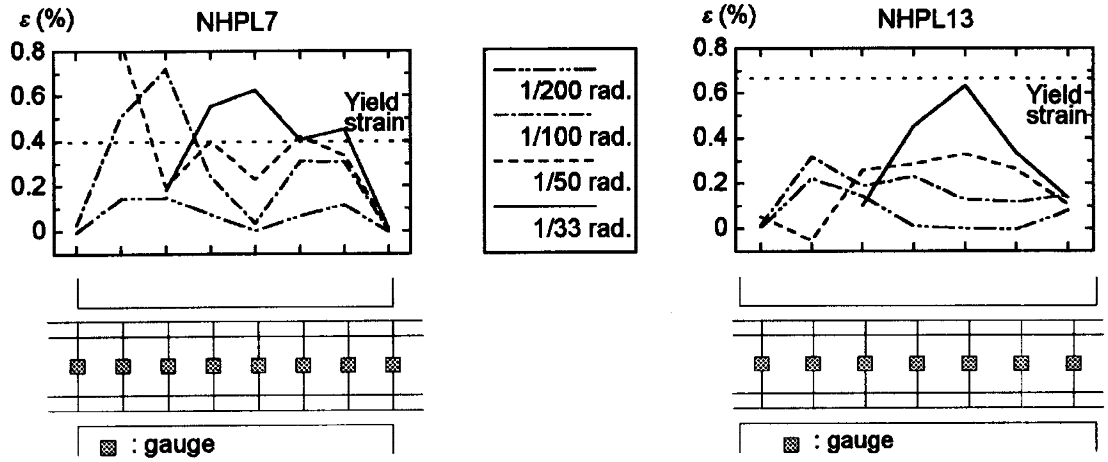

Fig. 6 Strain distribution of stirrups at the peak loads

DISCUSSIONS

Capacity Indexes and Ductility of Short Span Beams

Test results indicate that the ductility has better relationship with the failure modes. Fig. 7 shows the relationship between capacity indexes and failure modes. The left side shows the relationship between shear capacity index and failure mode (ST, SC, BO and only F), and the right side shows the case of bond capacity index. Circles indicate the specimens with shear span ratio (*M/QD*) of 1.2, and squares indicate of 1.4. From the left side graph, it is recognized that the failure mode changes from ST to SC and F as the value of shear capacity index increases in spite of differences of shear span ratio and / or concrete type. However, specimens failed by BO have large range of shear capacity index. On the other hand, bond capacity index has no correlation with failure mode. These results lead that the critical ductility angle may be determined by the value of shear capacity index.

The relationships between capacity indexes and critical ductility angles are shown in Fig. 8. The left side also shows the case of shear capacity index and the right side is of bond capacity index. From the left side graph, it is clearly regarded that the critical ductility angle has a proportional correlation with shear capacity index. Following formula is obtained from the regression analysis:

$$ {}_{e}R_{u} = 0.0568 \cdot {}_{c}Q_{su} / {}_{c}Q_{mu} - 0.0393 \quad [1] $$

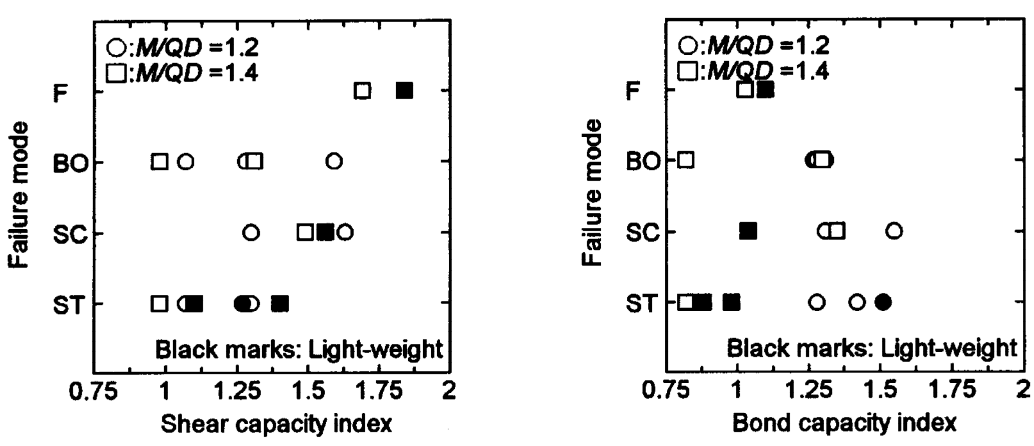

Fig. 7 Relationship between capacity index and failure mode

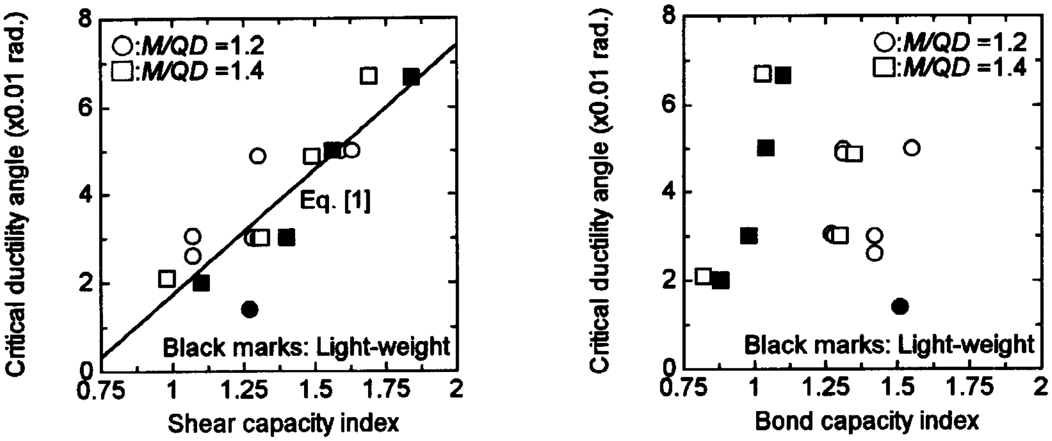

Fig. 8 Relationship between capacity index and critical ductility angle

where,

${}_{e}R_{u}$: critical ductility angle (radian)

${}_{c}Q_{su} / {}_{c}Q_{mu}$: shear capacity index

${}_{c}Q_{su}$: calculated shear strength

${}_{c}Q_{mu}$: calculated bending strength

The critical ductility angle of short span RC beams can be predicted by using this formula. On the other hand, bond capacity index has no relationship with critical ductility angle.

The authors have already tested ordinary span RC beams, which have shear span ratio of 2.0 (Sonobe et al., 1992). These specimens had also 800 MPa class stirrups, and normal weight concrete of 36 MPa class was also cast. Test programs for these specimens are the same as this research. Fig. 9 shows the relationship between shear capacity index and critical ductility angle including the test results of these specimens with shear span ratio of 2.0. Some specimens are plotted horizontally at the Y-axis value of 0.07 radians, however, they did not decrease the load until the final loading stage. As shown in this figure, the marks are placed almost on the line in spite of deference of shear span ratio. Therefore, it is considered that the method to predict the critical ductility angle proposed in this study can be used for ordinary span beams.

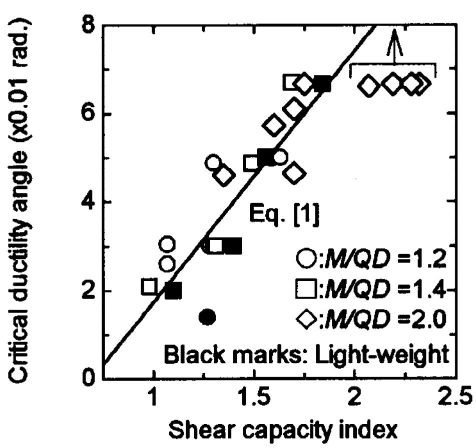

Fig. 9 Relationship between capacity index and critical ductility angle (including specimens with shear span ratio of 2.0)

CONCLUSIONS

1. Most specimens with shear span ratio of 1.2 or 1.4 fail after yielding of longitudinal bars. Every specimens did not show a decrement of the load until R =1/50 radians. Especially, specimens reinforced with diagonal longitudinal bars show a ductile behavior.
2. Three types of failure modes are observed. Those are shear failure, shear compression failure and bond splitting failure. The critical ductility angle has better relationship with failure modes.
3. The stress ranges of stirrups are 600 - 800 MPa in specimens used for this research.
4. Shear capacity index and bond capacity index are proposed for evaluating the ductility of RC beams. The shear capacity index has a good relationship with the critical ductility angle.
5. It is considered that the method to predict the critical ductility angle proposed in this study can be used for ordinary span RC beams.

ACKNOWLEDGEMENT

The authors gratefully acknowledge Tokyo Tekko Co., Ltd., Neturen Co., Ltd., Kotecs Co., Ltd. and Artificial Light-weight Aggregate Association. The authors also want to express their appreciation to Dr. H. Fukuyama, Senior Researcher of Building Research Institute, Ministry of Construction of Japan, and Mr. M. Ohyado, Researcher of Railway Technical Research Institute.

REFERRENCES

K. Mutoh (1967). Plastic Design of Reinforced Concrete Structures, Maruzen, Tokyo. (in Japanese)

Architectural Institute of Japan (1994). AIJ Structural Design Guidelines for Reinforced Concrete Buildings, pp. 77 - 91.

S. Morita and S. Fujii (1982). Bond Capacity of Deformed Bars Due to Splitting of Surrounding Concrete, Proceedings of the International Conference on Bond in Concrete, Paisley, Scotland.

Y. Sonobe, T. Kanakubo, M. Fujisawa and M. Ohyado (1992). Development on High Strength Reinforcement of Electric Furnace: Part6 Experimental Study on Ductility of Beams, Summaries of Technical Papers of Annual Meeting, Architectural Institute of Japan, C Structure II, pp. 505 - 506. (in Japanese)